Journal of the Physical Society of Japan
Vol. 54, No. 5, May, 1985, pp. 1823–1829

Effect of Current Density Profile on q(a) Limit in Non-Circular Tokamak TNT-A

Katsumi IDA,* Isao OCHIAI, Shunjiro SHINOHARA,
Yoshio NAGAYAMA, Hiroshi TOYAMA and Kenro MIYAMOTO

Department of Physics, Faculty of Science,
The University of Tokyo, Bunkyo-ku, Tokyo 113

(Received December 13, 1984)

The effect of the current density profile on the limit of the safety factor q(a) in the non-circular tokamak TNT-A is described in this paper. The safety factor q(a) is measured by magnetic probes and one-turn loops. The current density profile is estimated from the shape of the plasma boundary with an equilibrium code. A gas puffing system and pulse forming network (PFN) circuit for the Joule current are used to control the profile. The limit of q(a) increases from 2.6 to 4.0 as the current density profile becomes flatter and the current density profile parameter enters the unstable region for the $m=3$ and 4 external kink modes. This limit of q(a) determines one of the boundary of the operational stable region in TNT-A.

§1. Introduction

Research on stable discharges in tokamaks with low safety factor q(a) and high plasma density is important in order to obtain high β plasmas. The region of stable operation was studied in various tokamaks.[1,2] The boundary of the stable operation region is determined by the plasma density and the MHD instability. The MHD instability determines the limit of the safety factor (q(a) limit). To investigate the MHD instability in the vicinity of the q(a) limit, the current density profile was measured directly by magnetic probes in T-9[3] or was calculated from electron temperature profile $T_e(r)$ measured by Thomson scattering in DITE[4] and JIPP-T-II.[5] In a non-circular tokamak plasma, the current density profile, as well as the decay index and triangularity, is an important factor which is used to determine the elongation ratio. The relationship between the elongation ratio κ ($=b/a$: ratio of height to horizontal semi-axis length), triangularity γ and the decay index n_{index} ($=-(R/B_Z)(\partial B_Z/\partial R)$) was studied in Doublet III.[6]

In this paper, the stable operation region and the effect of the current density profile on the q(a) limit are described in a non-circular tokamak TNT-A.[7,8] To investigate this factor which determines the q(a) limit, the current density profile is estimated from the shape of the plasma cross section measured by magnetic probes and one-turn loops. An equilibrium code for a non-circular tokamak EQUCIR[9] is used to evaluate the current density profile. In addition, the current density profile is calculated from the T_e profile measured by Thomson scattering.

§2. Experimental Arrangement and Measurement

TNT-A is a non-circular tokamak with a major radius of 40 cm and a D-shape limiter, 36 cm high and 18 cm wide. The current in eight shaping coils (vertical field coils) and partial shell determines the decay index and elongated plasma cross section. The decay index is fixed to examine the effect of the current density profile on elongation ratio in this experiment. The plasma density is controlled by gas puffing. A pulse forming network (PFN) circuit for the Joule current is used to heat the outer plasma region. As shown in Fig. 1, the PFN circuit consists of six pairs of inductors and capacitors and is connected to the main

* Present address: Plasma Physica Laboratory, Princeton University, Princeton, New Jersey 08544, U.S.A.

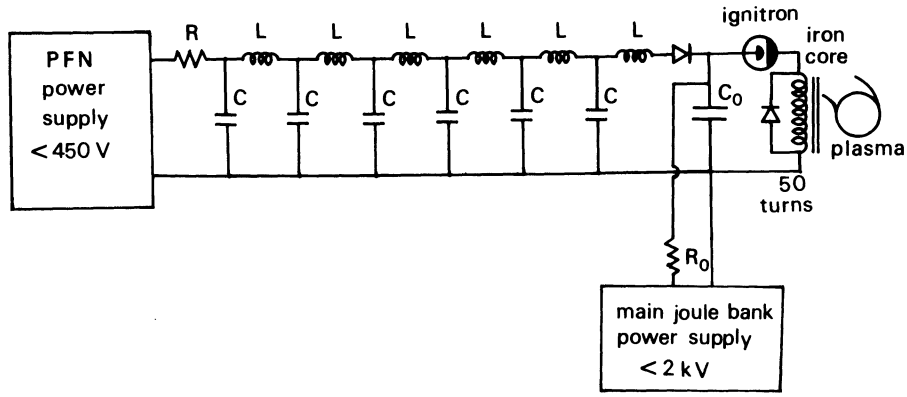

Fig. 1. Circuit diagram of the pulse forming network (PFN). Six pairs of inductors (L: 450 μH) and capacitors (C: 1.8 mF) are connected to a main bank (C_0: 1.4 mF).

bank. This circuit keeps the output voltage of the main bank constant. We can increase or decrease the plasma current by adjusting the voltage of the PFN power supply and, in combination with the gas puff, control the current density profile. The voltage is set much higher than 50 times the plasma loop voltage in order to increase the Joule input power. The PFN circuit is connected to the main bank when the plasma loop voltage goes down below 1/50 of the set voltage, usually 2~3 ms after the breakdown of discharge with the time constant of 7.7 ms. As we increase the plasma density with the gas puffing, we set the voltage higher to obtain the flatter electron temperature and current density profile. The heating suppresses shrinkage of the current channel due to cooling of the outer plasma region by gas puffing. Typical plasma current, loop voltage and plasma line-average density waveforms are shown in Fig. 2. The plasma current waveform has a flat top for a period of 10 ms. The electron temperature profile is measured by Thomson scattering at the time of the density flat top (t=10 ms) to calculate the current density profile. The toroidal magnetic field is up to 4.3 kG. The plasma suffers from major disruption caused by MHD instability at a plasma current $I_p = 10 \sim 20$ kA, and line-average density $\bar{n}_e = 0.5 \sim 1.5 \times 10^{13}$ cm^{-3}.

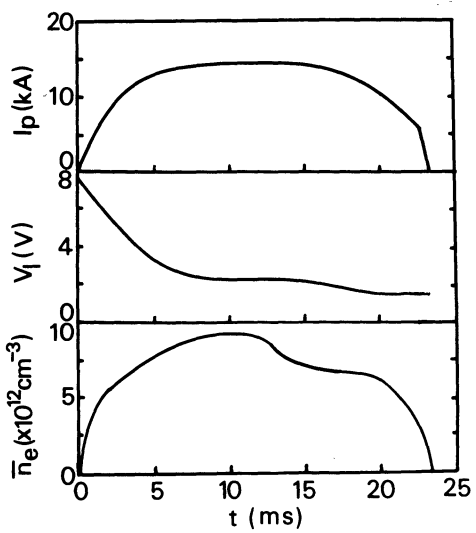

Fig. 2. Typical plasma current, loop voltage and plasma line-average density waveforms produced by the PFN and gas puffing.

The shape of the plasma cross section is calculated from the magnetic field and the flux, measured with 12 pairs of magnetic probes and 9 one-turn loops located in the shadow of the limiter. Using a simple flux function[10] the shape of the plasma cross section (triangularity γ, elongation ratio κ), the circumference of plasma boundary L_a and the position of plasma center are obtained as a function of time. The safety factor q(a) is evaluated using the following equation,

$$q(\mathrm{a}) = \frac{L_a^2 B_t}{2\pi\mu_0 R I_p}, \tag{1}$$

where R, B_t and I_p are major radius, toroidal magnetic field and plasma current, respectively. The electron temperature is measured by Thomson scattering at several vertical locations (-6.0 cm $< z <$ 6.0 cm) to obtain the profile.

§3. Experimental Results

3.1 Region of stable operation and elongation ratio

The stable operation region of TNT-A in $1/q(a)$, $\bar{n}_e/(B_t/R)$ parameter space has three types of boundary as shown in Fig. 3. Boundaries (A), (B) and (C) are determined by low density limit, MHD instability (q(a) limit), and high density limit, respectively. The boundary (A) gives a minimum density which is not reduced by lowering gas puffing. At boundary (B), the plasma current suffers from major disruption. The limit of safety factor q(a) depends on the line-average density, which is controlled by gas puffing and the plasma current waveform. At this boundary, the q(a) limit increases from 2 to 4 as the line-average density is increased. The effective ion charge estimated from the plasma resistivity and the electron temperature profile is between 1.8 and 2.1. This boundary is determined by the current density profile as described in Section 3.3. The electron temperature decreases rapidly and the discharge becomes resistive when the parameters of the operating region are close to the boundary (C). We deal with the boundary (B) in this paper.

A scan of plasma density was performed with a constant plasma current and n_{index} to examine the operational dependence of the elongation

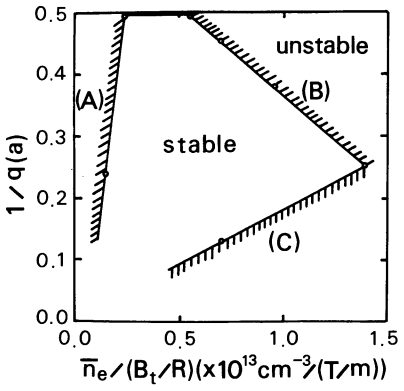

Fig. 3. Region of stable operation in $1/q$(a), $\bar{n}_e/(B_t/R)$ parameter space in TNT-A. Open circles show the inverse safety factor and the normalized line-average density immediately before the disruption, which happens at boundary (B). The boundary (A) gives a minimum density which is not reduced by lowering gas putting. The electron temperature decreases rapidly at boundary (C).

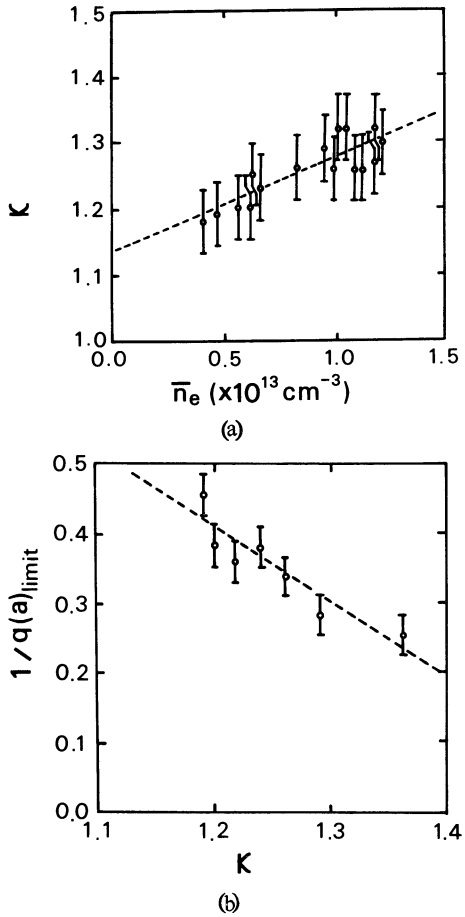

Fig. 4. Elongation ratio and limit of the safety factor at different values of line-average density. Open circles are experimental results measured with magnetic probes and one-turn loops. The dashed line is determined by the least squares method. (a) Elongation ratio as function of line-average density for $n_{index}=-0.8$, triangularity $\gamma=0.3$ and $q(a)=3\sim4$. (b) Limit of safety factor $q(a)_{limit}$ as a function of elongation ratio for $n_{index}=-0.8$, triangularity $\gamma=0.3$. The limit of safety factor $q(a)_{limit}$ and elongation ratio are measured immediately before disruption of the plasma current.

ratio on the plasma density. In this scan, the voltage of PFN is adjusted to get the same plasma current with different plasma density. As is shown in Fig. 4(a), the elongation ratio increases from 1.2 to 1.3 as line-average density is increased. This scan indicates that the plasma is more elongated in higher plasma density and larger Joule input even with a constant n_{index} value ($=-0.8$) in TNT-A. The elongation ratio of the plasma is controlled indirectly with the gas puffing and the PFN

circuit at the fixed n_{index} value, from the operational point of view. In physics, the higher elongation is due to the flatter current density profile as described in Sec 3.2. Figure 4(b) shows the limits of inverse safety factor $1/q(a)_{limit}$ with various elongation ratio [with various plasma density as known in Fig. 4(a)]) at the fixed toroidal field and n_{index} ($=-0.8$). The limit of the safety factor increases from 2.2 to 4.0 as the elongation ratio is increased. These $q(a)$ limits provide the boundary (B) of the stable discharge region in Fig. 3. As the line-average density is increased with gas puffing the current density profile becomes flatter and the gradient of current density near plasma boundary becomes larger. The large gradient of current density causes the enhancement of $m=3$ and 4 external kink modes instability and increases the $q(a)$ limit. The details of the instability are described in Sec. 3.3. The PFN circuit has the role to suppress the narrowing of the current channel and provides the flatter electron temperature and current density profile and higher elongation ratio in the higher density plasma. The current density profile can be controlled by the combination of gas puffing and the PFN circuit, and the profile has an effect on $q(a)$ limit.

3.2 Elongation ratio and current density profile

The elongation ratio is a function of triangularity, decay index and current density profile. The plasma β is low ($\sim 0.2\%$) enough that it can be assumed to have no sensitive effect on plasma equilibrium. Decay index is determined from the configuration of shaping current flowing in eight shaping coils, and triangularity is approximately constant in TNT-A. The elongation ratio is determined from the current density profile. To obtain the relationship between the elongation ratio and the current density profile, it is necessary to evaluate the profile shape at the $q(a)$ limit. The relationship is obtained from the equilibrium code EQUCIR. The elongation ratio is measured by magnetic probes and loops, and the electron temperature profile is measured with Thomson scattering to check the suitability of the equilibrium code for TNT-A. The profile parameter α of T_e is defined by the following equation,

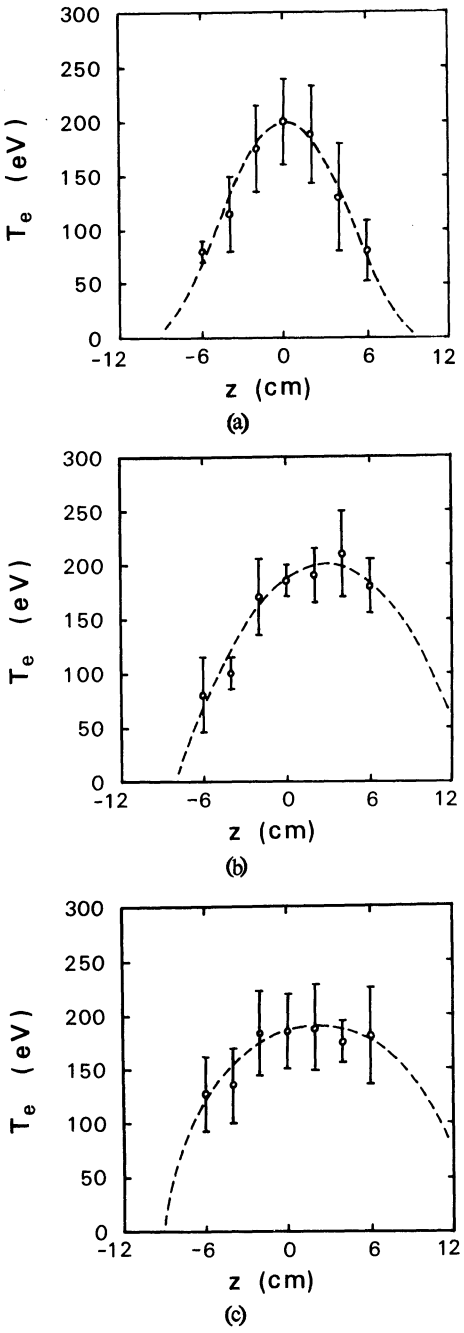

Fig. 5. Vertical dependence of electron temperature. Open circles are the result of Thomson scattering by laser, and dashed lines are $T_e=T_e(\text{center})(1-(z-z_0)^2/b^2)^\alpha$ determined by the least squares method. (a) Peaked profile without gas puffing for elongation ratio $\kappa=1.16$, and fitting profile parameter $\alpha=2.5$. (b) Rounded profile with weak gas puffing for elongation ratio $\kappa=1.24$, and fitting profile parameter $\alpha=1.2$. (c) Flattened profile with strong gas puffing for elongation ratio $\kappa=1.26$ and fitting profile parameter $\alpha=0.6$.

$$T_e(z)=T_e(\text{center})(1-(z-z_0)^2/b^2)^\alpha, \quad (2)$$

where z_0 is the vertical shift due to the field curvature and b is the vertical semi axis length. The location of the plasma edge is determined by the magnetic surface which goes through the limiter. The electron temperature of the plasma edge is estimated to be 5 eV ~ 10 eV from the measurements of electric probes. The value of the parameters T_e (center) and α are determined by the least squares method using measured values. The electron temperature profile can be changed by control of the gas puffing and PFN circuit as is shown in Fig. 5(a)–(c). Figure 5(a) shows a peaked electron temperature profile without gas puffing and with the PFN at low voltage which is not enough to heat the plasma boundary. Figure 5(b) shows a rounded temperature profile with weak gas puffing and sufficient PFN Joule input. The combination of the strong gas puffing and the PFN input at very high set voltage provides a flattened temperature profile as shown in Fig. 5(c). In these discharges, the toroidal filed $B_t \sim 3.5$ kG and the safety factor $q(a) \sim 4$. The profile parameter of T_e decreases from 2.5 to 0.6 and the elongation ratio increases from 1.16 to 1.26 as gas puffing becomes stronger.

The current density profile is calculated from the T_e profile assuming that $j(z) \propto T_e(z)^{3/2}$ during the flat top of plasma current. The relationship between elongation ratio and the current density profile parameter ν ($=1.5\alpha$) is shown in Fig. 6. The vertical axis is the elongation ratio measured by magnetic probes and one-turn loops. The horizontal axis is the current density profile parameter derived from the electron temperature. The solid line is the curve calculated by EQUCIR code and the calculated values agree with experimental ones. The parameters used in this calculation are $\gamma=0.3$ and $n_{\text{index}}=-0.8$, in the case where the decay index and triangularity are known, the current density profile is obtained from the elongation ratio without T_e profile measurement. Because the shape of the plasma cross section is measured only with magnetic probes and one-turn loops, the elongation ratio, as well as the triangularity, can be obtained even immediately before a major disruption. The current profile at the q(a) limit can be calculated from the elongation ratio.

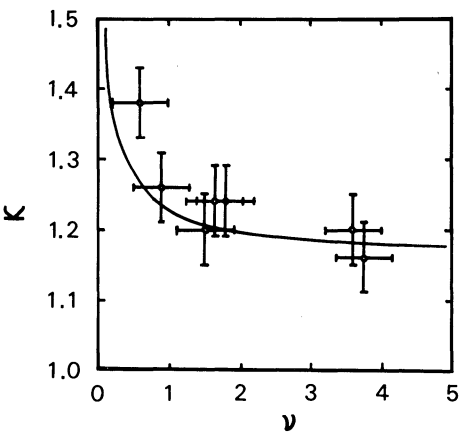

Fig. 6. Elongation ratio as a function of current density profile parameter. Open circles are the result of magnetic probes and one-turn loop and Thomson scattering, and solid line is the theoretical curve calculated with EQUCIR code for the plasma $\beta=0.2\%$, $n_{\text{index}}=-0.8$ and triangularity $\gamma=0.3$.

3.3 *Limit of safety factor q(a)*

The plasma suffers disruption as the current density profile becomes broader. Tearing modes are measured by Mirnov coils. In TNT-A, the poloidal field fluctuation[11] is still less than 1% for $m=3$ and 4 modes and 0.5% for $m=2$ mode even immediately before the disruption. Thus tearing modes are considered to have no role in disruptions for this experiment. Kink modes are not measurable, because the growth time is too short (~ 0.2 μs) compared to the period of the fluctuation (~ 30 μs). The dependence of the q(a) limit on the current density profile is shown in Fig. 7. The horizontal axis is the profile parameter calculated from the value of the elongation ratio by using the calculational curve in Fig. 6. Experimental data shows that the limit of q(a) increases from 2.6 to 4.0 as the profile parameter decreases from 0.8 to 0.2.

The unstable region of ideal external and internal kink modes[12] are also shown in Fig. 7. The profile parameter $\nu > 1$ is necessary for stability with free boundary (without conductive wall). An additional sawteeth unstable region appears on the basic $\nu=1$ stability boundary with effect of finite mode number m.

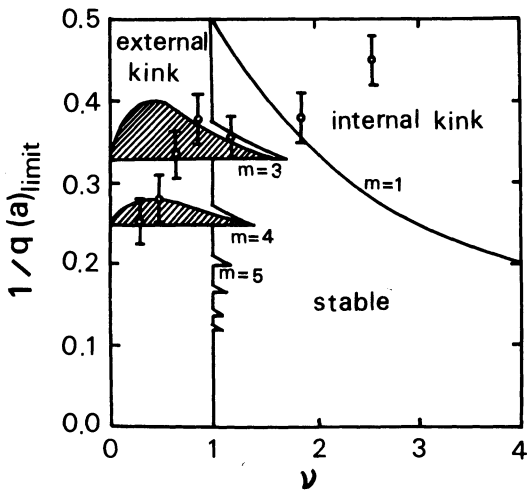

Fig. 7. Limit of inverse safety factor $1/q(a)_{limit}$ as a function of the current density profile parameter. Open circles are the result of calculations taken from the values of the elongation ratio in Fig. 4(b), by using calculational curve shown in Fig. 6. Left and upper unstable region shows the ideal external and internal kink mode, respectively. Poloidal mode number m are indicated in the figure. The shadow areas indicate the region which remain unstable if there is a perfectly conducting wall at the location of $2a$ (a: plasma radius) for $m=3$ and $m=4$.

When the profile parameter decreases to the unstable region in which the ideal kink mode is enhanced, the plasma current suffers a major disruption. The stable region determined by our experiment is wider than that from theory because of the effect of the conductive wall. When the wall is very close to the plasma boundary, the external kink mode is completely suppressed. In the case of TNT-A, the cross section of the plasma is D-shape, 18 cm wide and 22 cm hight. The vessel has the rectangular cross section, 24 cm wide and 60 cm high. The ratio of plasma radius to wall radius is 1.3 (horizontally) and 2.7 (vertically). Because the wall is located at a distance from the plasma boundary in the vertical direction, the external kink mode is not completely suppressed.

The shadow areas indicate the region which remain unstable if there is a perfectly conducting wall at the location of $2a$ (a: plasma radius). The boundary of this theoretical unstable region agrees with experimental data at the time of disruption on the boundary (B) in Fig. 3 in TNT-A, whose conducting wall is located far from plasma boundary (effective wall radius is twice as large as plasma minor radius). When the profile parameter is in the range, $\nu=0.6\sim1.2$, the $m=3$ external kink mode determines the q(a) limit, and the effect of higher kink modes ($m>3$) is neglected because the higher modes have smaller growth rates. As the profile parameter is decreased, the plasma is more unstable for the kink mode and $m=4$ kink mode ($\nu=0.2\sim0.4$) determines the q(a) limit.

§4. Conclusion

The current density profile is calculated from the shape of the plasma cross section (elongation ratio κ and triangularity γ) with the equilibrium code EQUCIR. Suitability of the code for TNT-A is confirmed by the agreement of experimental values and calculated ones in the relationship between elongation ratio and the profile shape parameter. The current density profile parameter at the q(a) limit is estimated from the elongation ratio immediately before the major disruption. This method is more convenient than evaluation from T_e profile measured by Thomson scattering, since the measurement of elongation ratio is possible even immediately before a major disruption. It is difficult to measure the T_e profile by Thomson scattering immediately before a major disruption, because it is unknown when the disruption will occur. The limit of $1/q$(a) decreases as the current density profile becomes flatter and the profile parameter enters the parameter region where the $m=3$ and 4 external kink modes are enhanced. These q(a) limits determine the boundary (B) of the operational stable region in Fig. 3. The agreement of the experimental boundary (B) with theoretical one in Fig. 7 explains that this boundary is due to $m=3$ and 4 external kink mode instability.

Acknowledgment

We would like to express our appreciation to Dr. S. Tsuji and Mr. K. Yamagishi for their assistance in the preparation of the experimental system, Mr. Y. Kimura for his assistance in preparing the gas puffing system, and Mr. Y. Ohki for his helpful discussions.

References

1) S. J. Fielding, J. Hugill, G. M. McCracken, J. W. M. Paul, R. Prentice and P. E. Stott: Nucl. Fusion **17** (1977) 1382.
2) M. Nagami, H. Yoshida, K. Shinya, G L. Jahns, H. Yokomizo, M. Shimada, K. Ioki, S. Izumi and A. Kitsunezaki: Nucl. Fusion **22** (1983) 409.
3) A. V. Bortnikov, N. N. Brevnov, S. N. Gerasimov, V. G. Zhukovskii, V. I. Pergament and L. N. Kimchenko: Sov. J. Plasma Phys. **3** (1977) 110.
4) K. B. Axon, G. A. Baxter, J. Burt, W. H. M. Clark, G. M. McCracken, S. M. Fielding, R. D. Gill, D. H. J. Goodall, M. Hobby, J. Hugill, J. W. M. Paul, B. A. Powell, R. Prentice, G. W. Reid, P. E. Stott, D. D. R. Summers and A. J. Wooton: in *Plasma Physics and Controlled Nuclear Fusion Research (Proc. 7th Conf. In-sbruck, 1978)* **1**, (IAEA, Vienna, 1979) p. 51.
5) K. Toi, S. Itoh, K. Kadota, K. Kawahata, N. Noda, K. Sakurai, K. Sato, S. Tanahashi and S. Yasue: Nucl. Fusion **19** (1979) 1643.
6) H. Yokomizo, M. Nagami, M. Shimada, M. Maeno, H. Yoshida, K. Shinya, K. Ioki, S. Izumi, P. Rock, N. H. Brooks, R. Seraydarian, N. Fujisawa and A. Kitsunezaki: Nucl. Fusion **22** (1982) 797.
7) S. Shinohara, K. Sakuma, Y. Nagayama and H. Toyama: J. Phys. Soc. Jpn. **52** (1983) 94.
8) H. Toyama, A. Iwahashi, H. Kaneko, Y. Kawada, K. Makishima, Y. Nagayama, I. Ochiai, K. Sakuma, S. Shinohara, S. Tsuji, Y. Tsuji, K. Yamagishi, T. Dodo, O. Okada, T. Kuroda, Y. Oka, T. Okada, Y. Tanaka, S. Takamura, K. Sakaurai, K. Nakamura, T. Kuzushima, H. Matsushita, U. Suzuki and Y. Uesugi: in *Plasma Physics and Controlled Nuclear Fusion Research (Proc. 7th Conf. Innsbruck, 1978)* **1**, (IAEA, Vienna, 1979) p. 365.
9) H. Ninomiya, K. Shinya and A. Kameari: *Proc. 8th Sympo. on Engineering Problems of Fusion Research*, **1** (1979) p. 75.
10) K. Idà and H. Toyama: J. Appl. Phys. **22** (1983) 1589.
11) S. Shinohara, I. Ochiai, S. Tsuji, H. Toyama and K. Miyamoto: J. Phys. Soc. Jpn. **52** (1983) 364.
12) J. A. Wesson: *Controled Fusion and Plasma Physics* 2 (1975) p. 102.